Chapter 4

Polarized Backlights Using Sub-wavelength Grating

As applications for thin-film transistor (TFT) LCD's grow, bright and uniform backlight modules become essential. The optical efficiency of conventional backlight modules is low due to the lack of p-polarized to s-polarized light conversion (P-S conversion). In addition, the complex assembling of optical films, such as Brightness Enhancement Film (BEF), Dual Brightness Enhancement Film (DBEF) and diffuser, usually hinders compact packaging. Many methods have been reported to separate polarized light, thus, producing uni-polarized light to enhance polarization conversion efficiency. In a previous design, a polarized backlight used micro structures at the Brewster angle to produce uni-polarized light.[1] However, the polarization efficiency is strongly dependent on the incident angles of light. In addition, a stack of multilayered thin films (alternating layers of materials of high and low refraction indices) was designed to match a quarter-wave optical thickness in each layer. So that Brewster condition was satisfied to produce specific polarized state of light.[2] However, the tolerances in incident angle and wavelength are very limited. In this chapter, a polarized backlight using sub-wavelength grating was proposed to achieve polarization conversion and compactness for LCD illumination.

4.1 Principle of Polarized Backlights Using Sub-wavelength Grating

When unpolarized light was coupled to the lightguide, slot structures on the backside of lightguide make light be extracted as shown in Fig. 4-1. Light was then

reflected by the reflective sheet. Upon the impingement on the sub-wavelength grating on the front side, only p-polarized light was transmitted while s-polarized light was reflected. S-polarized light was then converted into p-polarized light by passing through the quarter wave plate twice. In addition, the sub-wavelength grating is less critical on incident angle. Therefore, outcoupling light was uni-polarized, which was required for LCD illumination.[3]
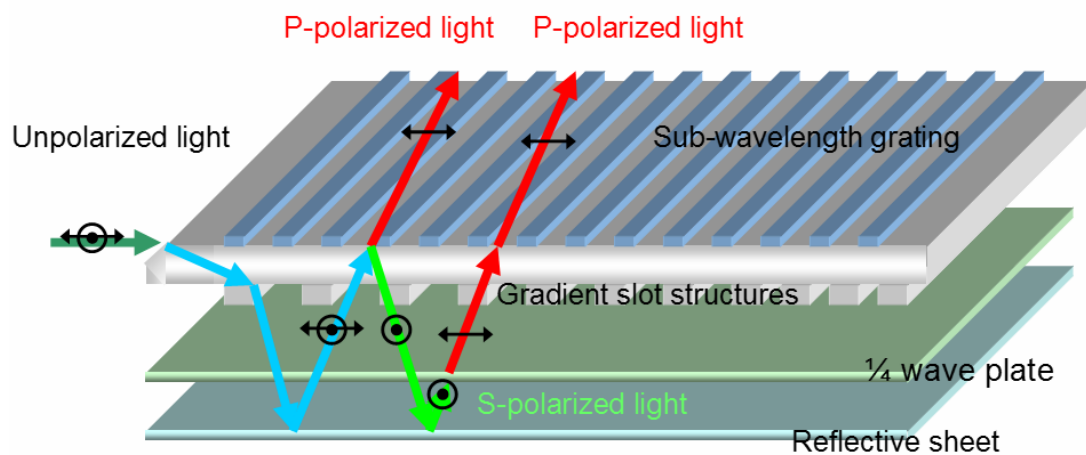

Fig. 4-1. Schematics of polarized backlights using sub-wavelength grating. P-polarized light is transmitted while s-polarized light is reflected. S-polarized light is then converted into p-polarized light by passing through the quarter wave plate twice.

4.1.1 Theory of the Sub-wavelength Grating

Characteristics of birefringence are essential to separate s-polarized and p-polarized light. In addition to asymmetry of material or incident angle, variation of interface profile is another way to produce asymmetry. In a surface relief grating, for example, it is obvious that s-polarized and p-polarized light encounter different boundary conditions at the interface. Sub-wavelength grating is a special case of gratings, which produces polarization separation effect. The relationship between the period of diffraction grating and wavelength of incident light is given by the following equation

$$p\left(n_i \sin\theta_i + n_d \sin\theta_d\right) = m\lambda \qquad (4\text{-}1)$$

where p is the period of grating; n_i and n_d are the refractive indices of media where incident light and diffraction light exist; θ_i and θ_d correspond to the incident angle and diffraction angle, respectively; m is the diffraction order and is an integer.[4] When the condition:

$$p < \frac{\lambda}{\left(n_i \sin\theta_i + n_d\right)} \qquad (4\text{-}2)$$

is satisfied, we find that all diffraction orders but the zeroth order are evanescent, i.e., they yield diffraction angle $\theta_d > 90°$. Hence the grating is also called zero-order grating.[5][6] If the period p of the grating is sufficiently small compared to the wavelength, the whole structure behaves as if it were homogenous and uniaxially anisotropic, which is namely form-birefringence.[7]

Limited by the condition above, the sub-wavelength grating behaves no more as a grating, but as an effective dielectric medium with corresponding refractive indices, $n_{//}$ and $n_{\perp}$. Two orthogonal polarized light encounters different effective refractive indices due to the asymmetric grating structure, one parallel to the grating (s-polarized light) and the other perpendicular to the grating (p-polarized light). Considering a 1D grating composed of two materials of refractive indices n_1 and n_2, with a duty cycle f, the effective indices are given by the formulas[8]:

$$n_{//} = [f \times n_1^2 + (1-f) \times n_2^2]^{1/2} \qquad (4\text{-}3)$$

$$n_{\perp} = n_1 \times n_2 \times [f \times n_2^2 + (1-f) \times n_1^2]^{-1/2} \qquad (4\text{-}4)$$

Therefore, for a grating with period smaller than wavelength of incident light, the unpolarized light will be separated, i.e., p-polarized light transmitted and s-polarized light reflected. However, the bandwidth of this kind sub-wavelength grating is usually narrow because of low efficiency in blue light spectrum. The efficiency of separating

polarized light of a sub-wavelength grating can be further increased by adopting multi-layered structure. In this thesis, the attention will be focused on the sub-wavelength grating with double-layered structure.
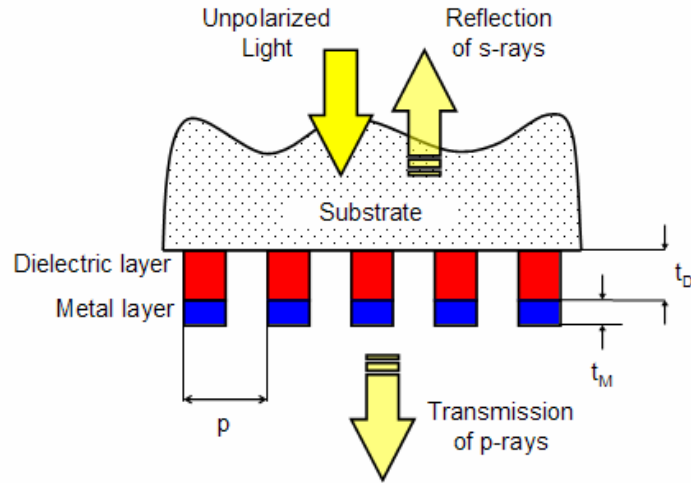

Fig. 4-2. Schematic structure of double-layered sub-wavelength grating.

Both effective refractive indices, $n_{//}$ and $n_{\perp}$, can be derived from the boundary conditions of Maxwell's equations. As schematically shown in Fig. 4-2, for s-polarized light, the relationship between effective refractive index $n_{//}$ and refractive indices of dielectric layer and metallic layer, n_D and n_M, is

$$n_{//}^2 = \frac{a}{P} n_M^2 + \frac{b}{P} n_D^2 \tag{4-5}$$

For p-polarized light, the relationship between effective refractive index $n_{\perp}$ and refractive indices of dielectric layer and metallic layer, n_D and n_M, is

$$\frac{1}{n_{\perp}^2} = \frac{a}{P \times n_M^2} + \frac{b}{P \times n_D^2} \tag{4-6}$$

Due to refractive index of metallic layer n_M is much larger than that of dielectric layer, Eqs. (4-5) and (4-6) can be approximated as

$$n_{//} \cong n_M \times \left(\frac{a}{P} \right)^{1/2} \tag{4-7}$$

52

and

$$n_\perp \cong n_D \times \left(\frac{b}{P}\right)^{-1/2} \tag{4-8}$$

Some interesting phenomena are noticed from Eqs. (4-7) and (4-8). When light is incident on the sub-wavelength grating, it is as if s-polarized and p-polarized light are incident on the metal layer and dielectric layer, respectively. Therefore, lots of s-polarized light is reflected with very high reflection efficiency and most of p-polarized light is transmitted.

4.2 Simulation

The lightguide model (8.8 cm wide, 7.1 cm long) was built by an optical simulation program to optimize the pattern design for achieving high uniformity. Slot structures and the sub-wavelength grating were fabricated on the backside and the front side of the lightguide, respectively.
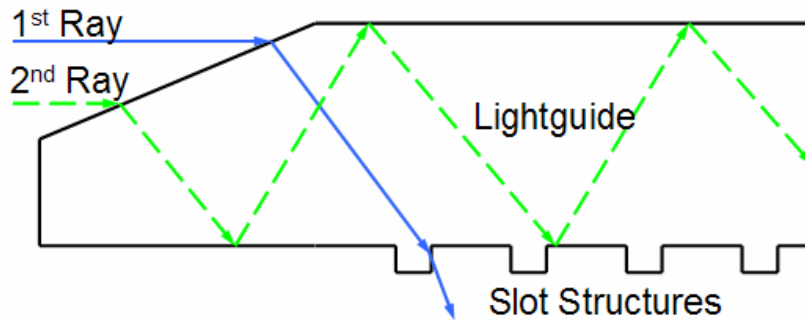

Fig. 4-3. Function of slot structures. The guided rays with oblique incidence were coupled out by the side walls of slot structures. The density of slot structures controlled uniformity on the outcoupling plane.

On the backside, slot structures were spaced in gradient, spacing more densely in the region far away from the light source and sparsely close to the light source.

When the light source was coupled into the lightguide by the slant surface, the trapped rays with oblique incidence were extracted by the side walls of slot structures, shown in Fig. 4-3. Slot structures determined the number of extracted rays and therefore the density of slot structures controlled uniformity on the outcoupling plane. Brightness profile on the outcoupling plane was obtained by ray tracing, as shown in Fig. 4-4. With a 650 lm white light source, the maximum and minimum values of illuminance are 43000 and 34000 lux, respectively. Uniformity of illuminance can achieve 80% over the active area (85 mm×70 mm) of the outcoupling plane, which is higher than required uniformity of 70% for commercial lightguide.
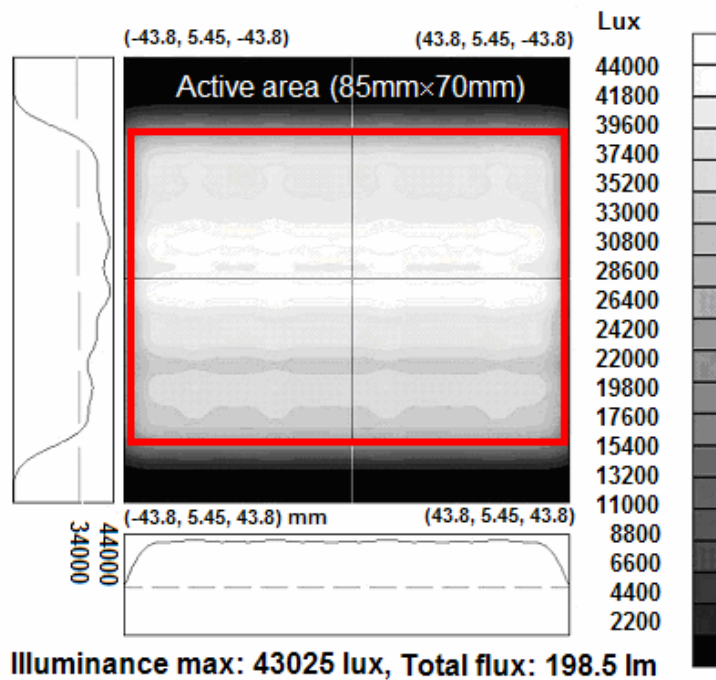

Fig. 4-4. Illuminance profile of the integrated lightguide. The maximum and minimum values of illuminance are 43000 and 34000 lux, respectively. Consequently, 80% of uniformity was then achieved.
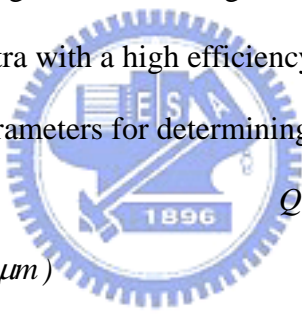
For accurately calculating the efficiency of p-polarized and s-polarized light, the package software, GSOLVER, is used to perform the simulation based on RCWA. According to Eqs. (4-5) and (4-6), the effective refractive indices of a sub-wavelength

grating are much dependent on its dimension and material. The sub-wavelength with smaller period produces a higher efficiency of light separation, but is harder to fabricate. To achieve high efficiency and easy fabrication simultaneously, the structure of the grating, including period, duty cycle, and thickness, has to be optimized. Thus, these parameters as well as material of the grating will be determined one by one in the following sections.

4.2.1 Period

Period of a grating is the most important parameter to determine the diffraction efficiency. Period is selected according to what kinds of applications will be applied. For example, form birefringence appears when the period of the grating is much smaller than the wavelength of incident light. Period of few sub-micrometers is needed to provide visible spectra with a high efficiency of light separation.

Tab. 4.1. Simulation parameters for determining period of metallic layer.

Substrate	*Quartz ($n = 1.54$)*
Period of grating (μm)	*0.1 ~ 0.3*
Duty cycle (%)	*50 (default value)*
Thickness of metallic layer (μm)	*0.1*
Material of metallic layer	*Aluminum*
Wavelength (μm)	*0.4 ~ 0.8*

In simulation, metallic layer, aluminum which is selected because of its high reflectivity, of the sub-wavelength grating with default setting of duty cycle is inserted in between quartz substrate and air. To consider the influence of incident angle of the incident light on diffraction efficiency, various incident angles are taken into account. After that, several periods of the sub-wavelength grating, which are selected to be smaller than visible spectra, are simulated with both p ray and s rays. The simulation

parameters are listed in Tab. 4.1.

It can be noticed that both p ray transmission and s ray reflection efficiency gradually become higher as the period of the sub-wavelength grating decreases as shown in Figs. 4-5 and 4-6. For the purpose of having the highest efficiency, the periods of the grating of 0.15 μm, 0.1 μm, or even smaller can be chosen. Nevertheless, the difficulty in fabrication is enormously increased as the period of the grating becomes smaller. In addition, a serious decay of p ray transmission appears in the shorter wavelength spectrum. The solution to avoid the steeply decay is to diminish the period or employ multi-layered structure, which will be discussed in detailed in section 4.3. Therefore, we trade-off the diffraction efficiency and limitation of fabrication instruments, and select period of the sub-wavelength grating to be 0.2 μm where p-polarized light transmission efficiency is about 80% and s-polarized light reflection efficiency is above 97% for the visible spectrum.
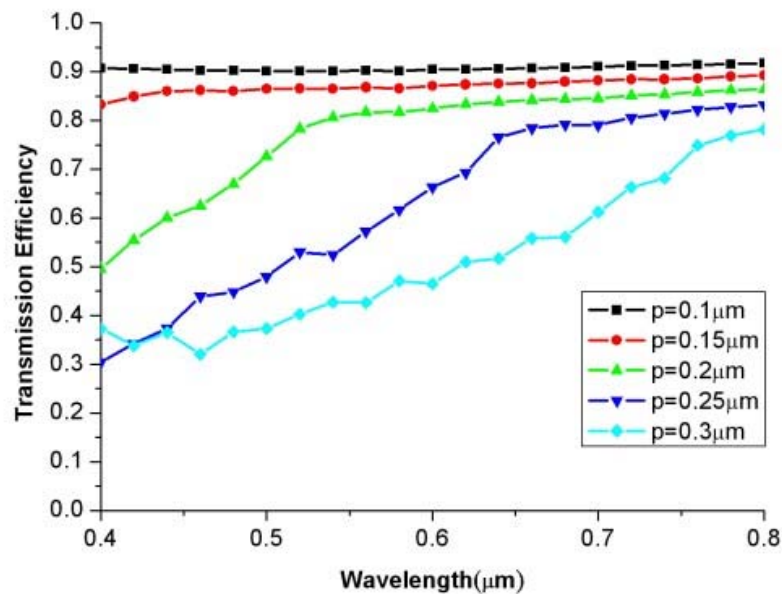
Fig. 4-5. Simulated results of p-polarized light transmission efficiency versus wavelength of incident light with various periods of the sub-wavelength grating.
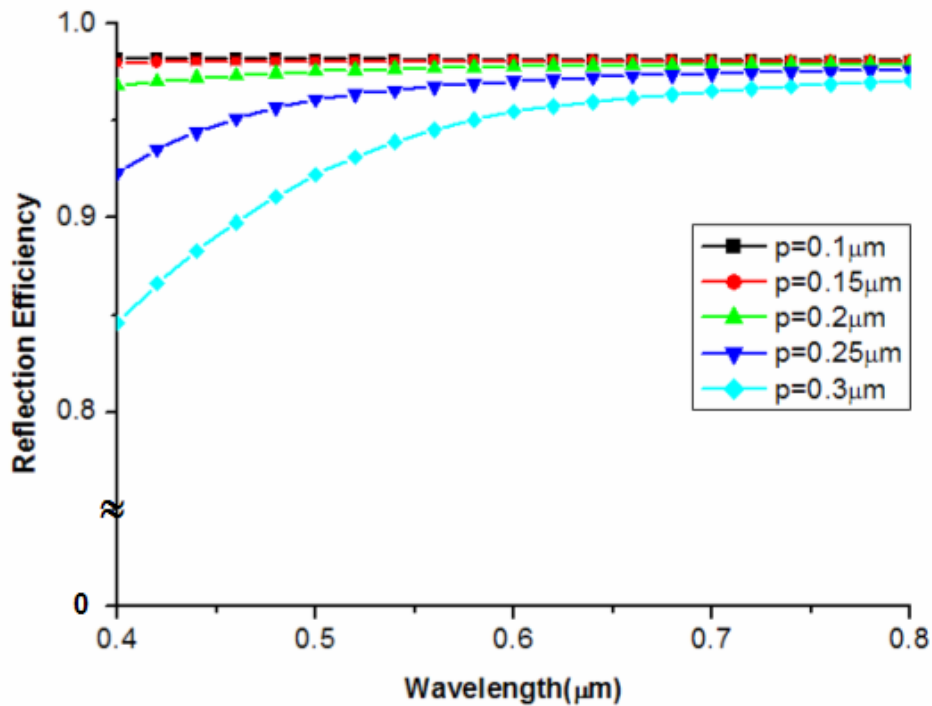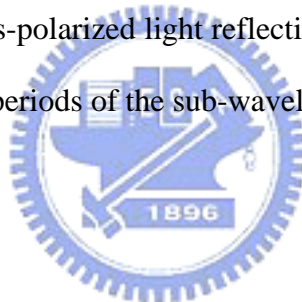
Fig. 4-6. Simulated results of s-polarized light reflection efficiency versus wavelength of incident light with various periods of the sub-wavelength grating.

4.2.2 Thickness

Various thicknesses of a diffraction grating result in a variation of amplitude or phase of incident wave, as well as the diffraction efficiencies. A proper thickness of the grating will enhance the diffraction efficiencies; on the contrary, an improper thickness will destroy the diffraction conditions and degrade the diffraction efficiencies. Thus, a suitable thickness of the metallic layer of the sub-wavelength grating needs to be tested.

In simulation, aluminum grating with well-chosen period and default setting of duty cycle of $0.2\,\mu m$ and 50%, respectively, is inserted in between quartz substrate and air. Afterwards, different thicknesses, range from $0.05\,\mu m$ to $0.2\,\mu m$, of the metallic layer are simulated with both p and s rays. The simulation parameters are listed in Tab. 4.2.

Tab. 4.2. Simulation parameters for determining thickness of metallic layer.

Substrate	*Quartz (n = 1.54)*
Period of grating (μm)	*0.2*
Duty cycle (%)	*50*
Thickness of metallic layer (μm)	*0.05 ~ 0.2*
Material of metallic layer	*Aluminum*
Polarization angle	*0˚ (s ray) & 90˚ (p ray)*
Wavelength (μm)	*0.4 ~ 0.8*

From the simulated results, both p ray transmission efficiency and s ray reflection efficiency are increased as thickness of metallic layer becomes thicker, as shown in Figs. 4-7 and 4-8.
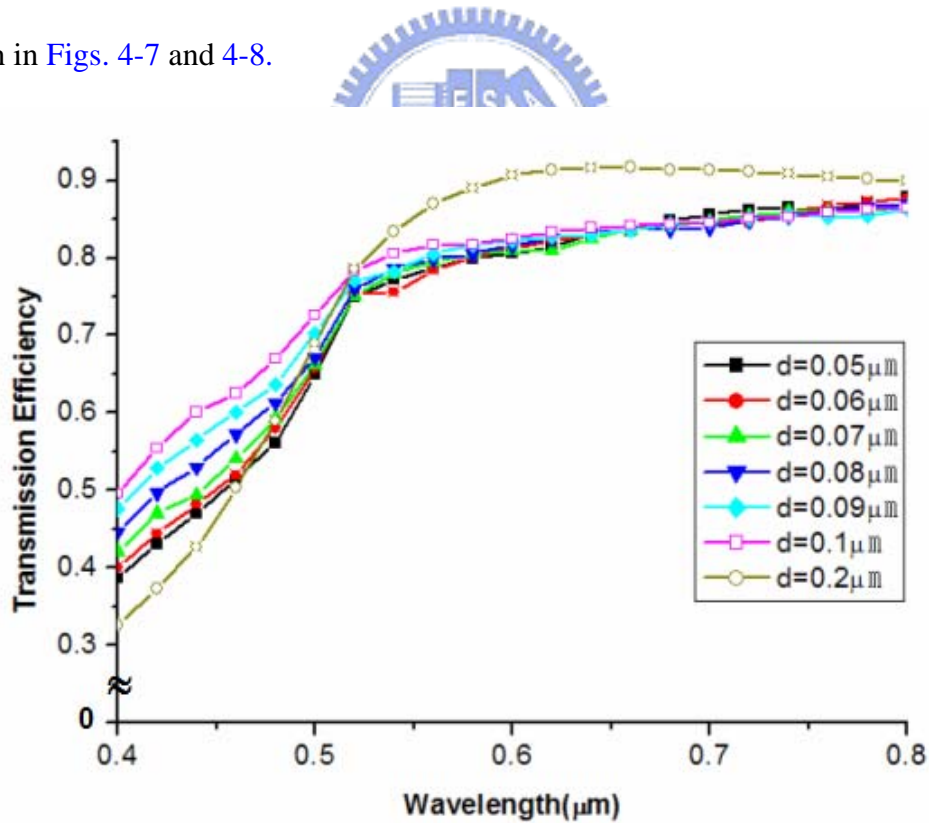

Fig. 4-7. Simulated results of p-polarized light transmission efficiency versus wavelength of incident light with various thicknesses of metallic layer.
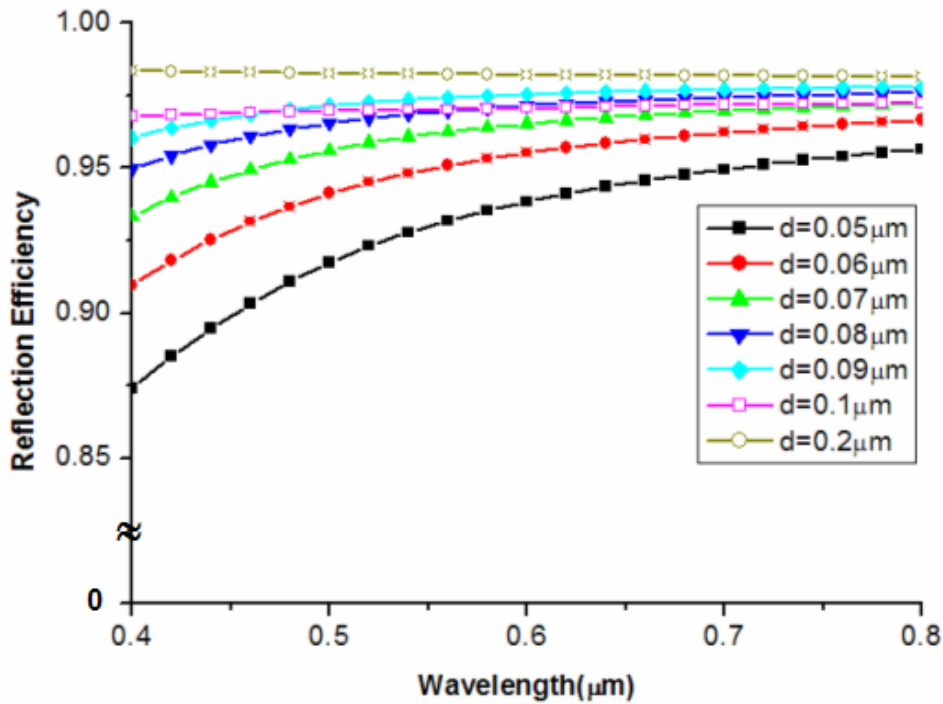
Fig. 4-8. Simulated results of s ray reflection efficiency versus wavelength of incident light with various thicknesses of metallic layer.

However, the p ray transmission efficiency with thickness larger than 0.1 μm is of a more serious decay in the region of shorter wavelength even if the diffraction efficiencies are higher. Furthermore, we expect that the thickness of the sub-wavelength grating can be as thin as possible to simplify the fabrication. Consequently, thickness of 0.1 μm, which is easier to fabricate and maintain p-polarized light transmission efficiency and s-polarized light reflection efficiency of 80% and 97% respectively, is selected.

4.3 Double-Layered Sub-Wavelength Grating

In the simulation of the sub-wavelength grating with metallic layer only, the efficiency of p-polarized light transmission is decreased rapidly in the shorter wavelength spectrum. The wavelength that the efficiency steeply decreases is the

so-called resonance wavelength. One of the methods to condense resonance wavelength, i.e., to broaden the applicable spectrum, is to design a sub-wavelength grating with multi-layered structure. Accordingly, a dielectric layer is added between aluminum layer and substrate to improve the decay of diffraction efficiency. The simulation of such a double-layered sub-wavelength grating will be demonstrated in the following.

4.3.1 Material of Dielectric Layer

First, the most suitable material of dielectric layer for our design was chosen. Metallic and dielectric layers with thickness of 0.1 μm and 0.2 μm, respectively, were inserted between quartz substrate and air once again. The same simulation conditions but different materials of dielectric layer were set to calculate the diffraction efficiencies with both p-polarized and s-polarized light. The simulation parameters were listed in Tab. 4.3.

Tab. 4.3. Simulation parameters for determining material of dielectric layer.

Substrate	*Quartz ($n = 1.54$)*
Period of grating (μm)	*0.2*
Duty cycle (%)	*50*
Thickness of metallic layer (μm)	*0.1*
Material of metallic layer	*Aluminum*
Thickness of dielectric layer (μm)	*0.2*
Material of dielectric layer	*MgO, SiO$_2$, ZnS*
Wavelength (μm)	*0.4 ~ 0.8*

From the calculated results, a monopolized curve, which is generated by utilizing SiO$_2$, of p ray transmission efficiency is acquired, as shown in Fig. 4-9, and nearly

identical curves of s ray reflection efficiency is obtained in Fig. 4-10. In consequence, SiO_2 is undoubtedly selected as the material of dielectric layer. Thus, the dielectric layer consists of SiO_2 with thickness of $0.2 \mu m$ is inserted between quartz substrate and metallic layer.
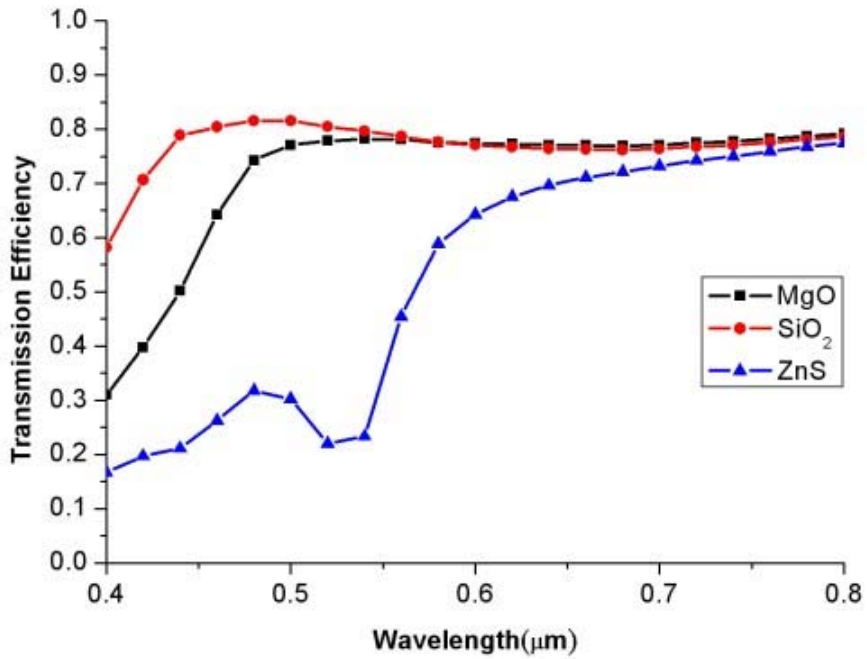

Fig. 4-9. Simulated results of p-polarized light transmission efficiency versus wavelength of incident light with various materials of dielectric layer.
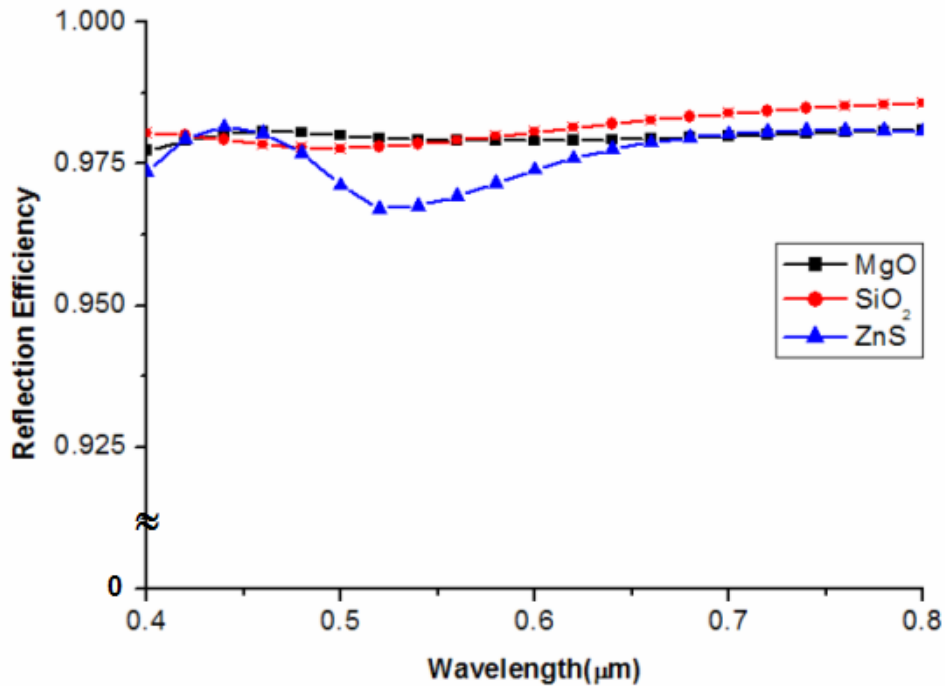
Fig. 4-10. Simulated results of s-polarized light reflection efficiency versus wavelength of incident light with various materials of dielectric layer.

In summary, a double-layered sub-wavelength grating which consists of a metallic layer and a dielectric layer has been designed. By optimizing both transmission and reflection efficiencies, the metallic layer, consists of aluminum, of the sub-wavelength grating with period, thickness, and duty cycle of $0.2 \, \mu m$, $0.1 \, \mu m$, and 50% respectively is obtained. In order to improve the steeply decay in the shorter wavelength spectrum of the transmission efficiency, i.e., to reduce the resonance wavelength, a dielectric layer, consists of SiO_2, is added between substrate and metallic layer. With this structure, most of p-polarized light can be transmitted through the sub-wavelength grating while s-polarized light is reflected, as shown in Figs. 4-11 and 4-12.
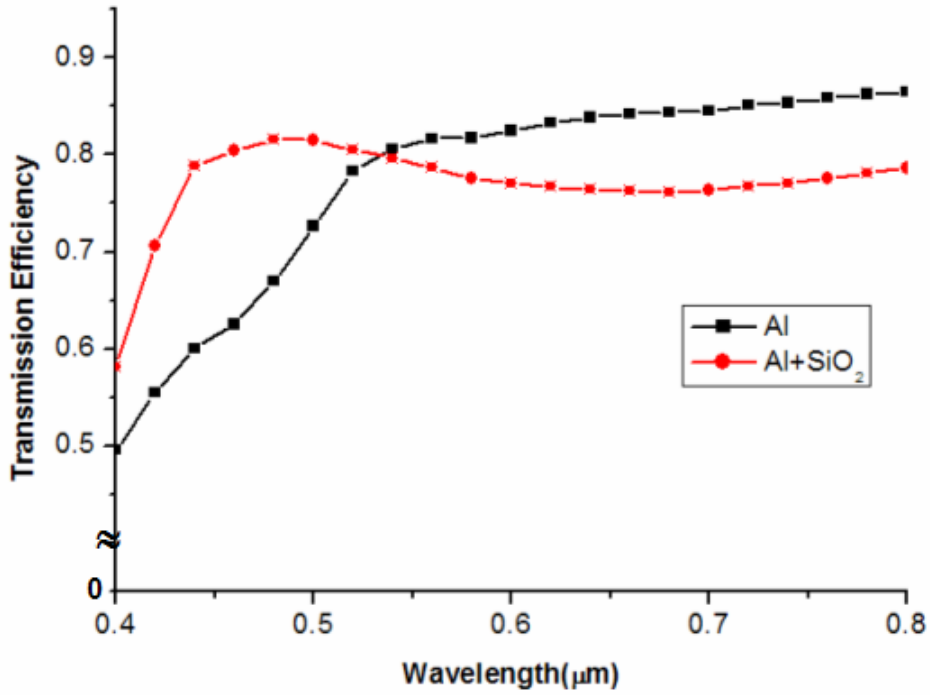
Fig. 4-11. Comparison of p-polarized light transmission efficiency between single layer and double layer.
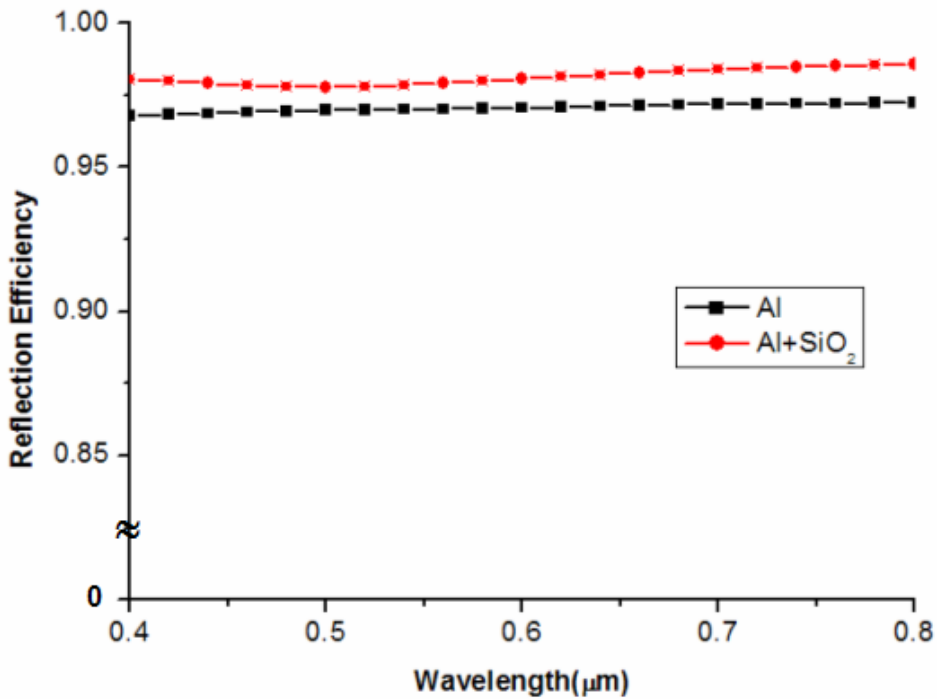

Fig. 4-12. Comparison of s-polarized light reflection efficiency between single layer and double layer.

4.4 Fabrication Technologies

Because the sub-wavelength grating interested in this thesis is mainly applied in display technologies, period of the sub-wavelength grating which is smaller than wavelength of visible spectrum, i.e. $0.4\,\mu m$ to $0.8\,\mu m$, is then essential. It is difficult to fabricate fine structures by utilizing general semiconductor process. High resolution electron beam lithography technology is therefore adopted for the easiness of fabricating sub-wavelength grating with fine structure.

4.4.1 Electron Beam Lithography (EBL) Technology

Electron beam lithography technology, employs high energy electron beams, is a specialized technique for creating the extremely fine patterns required by the modern electronics industry for integrated circuits, the academic research of physical and chemical properties of nanostructures, and the fabrication of mask used in semiconductor devices. Derived from the early scanning electron microscopes, the technique in brief consists of scanning a beam of electrons across a surface covered with a resist film sensitive to those electrons, thus depositing energy in the desired pattern in the resist film. The process of forming the beam of electrons and scanning it across a surface is very similar to CRT display mechanism, but EBL typically has three orders of magnitude higher in resolution. In the next section, two different fabrication processes of EBL for fabricating the sub-wavelength grating will be demonstrated. Besides, measurement systems used to evaluate the fabricated sub-wavelength grating will be also introduced in the last sections of this chapter.

4.4.2 Double-Layered Structure by Using Tri-Level Resist System

A tri-level resists system was then introduced to fabricate a double-layered

sub-wavelength grating. The detail steps for forming tri-level resist system and fabricating nanostructures were listed below：In the experiments, quartz wafer was the major substrate we would like to fabricate on.

(1) Wafer cleaning：First step was initially clean. It removed particles, which would affect the ultimately fabricated structure and its efficiency, from the wafer surface.

(2) PMMA/MMA coating：The coating of electron resist was applied. Substrates were placed on a vacuum chuck in the coater and the PMMA/MMA was dropped on to the wafer. A uniform and thin electron resist layer can be coated on the wafer surface after the wafer was spun by the coater. Thickness of PMMA/MMA depended on both concentration of PMMA/MMA solution and speed of coater. For example, a 3% PMMA/MMA solution was able to produce thickness of 100-1000 nm at speed of coater of 1000-5000 rpm for 60 seconds.

(3) Baking：The coated PMMA/MMA was baked on a hotplate at 160℃ for 15 minutes.

(4) Interlayer deposition：Because quartz wafer was not a conductor, electrons would accumulate on its surface during exposure. Such a phenomenon was so called *charge-up*. In order to avoid charge-up, Germanium was chosen as interlayer in the experiments. Besides being a conductive layer, it also served as an excellent mask for RIE in oxygen.

(5) Resist coating：The PMMA was spin coated on interlayer after interlayer was deposited.

(6) Baking：The coated PMMA was also baked on a hotplate at 160℃ for 15 minutes. Then, the tri-level resist system was formed.

(7) Exposure：The wafers were put into E-beam system after baking. The desired

patterns, line array with center-to-center distance of 0.2 μm in the experiments, were drawn by computer before exposure. Focusing electron beam was then controlled to scan the corresponding patterns on PMMA with certain of dosage.

(8) Development and Rinse：The exposed PMMA was developed for 75 seconds in 1:3 MIBK：IPA and rinse for 25 seconds in IPA. Then blow dry with nitrogen.

(9) RIE：RIE with CF_4 and oxygen was then applied sequentially to form a high aspect ratio resist profile.

(10) Materials evaporation：The desired structure was aluminum plus SiO_2. Thus, SiO_2 and aluminum were evaporated onto the sample sequentially by thermal evaporator.

(11) Lift-off：The samples were immersed into acetone for 15 minutes after removing from evaporator. Then we agitated substrates and acetone with an ultrasonic cleaner to dissolve the PMMA/MMA with its cover lift-off, and the desired nanostructure remained on the substrate.

The flow of fabricating sub-wavelength grating with double-layered structure by using tri-level resist system was shown in Fig. 4-13.
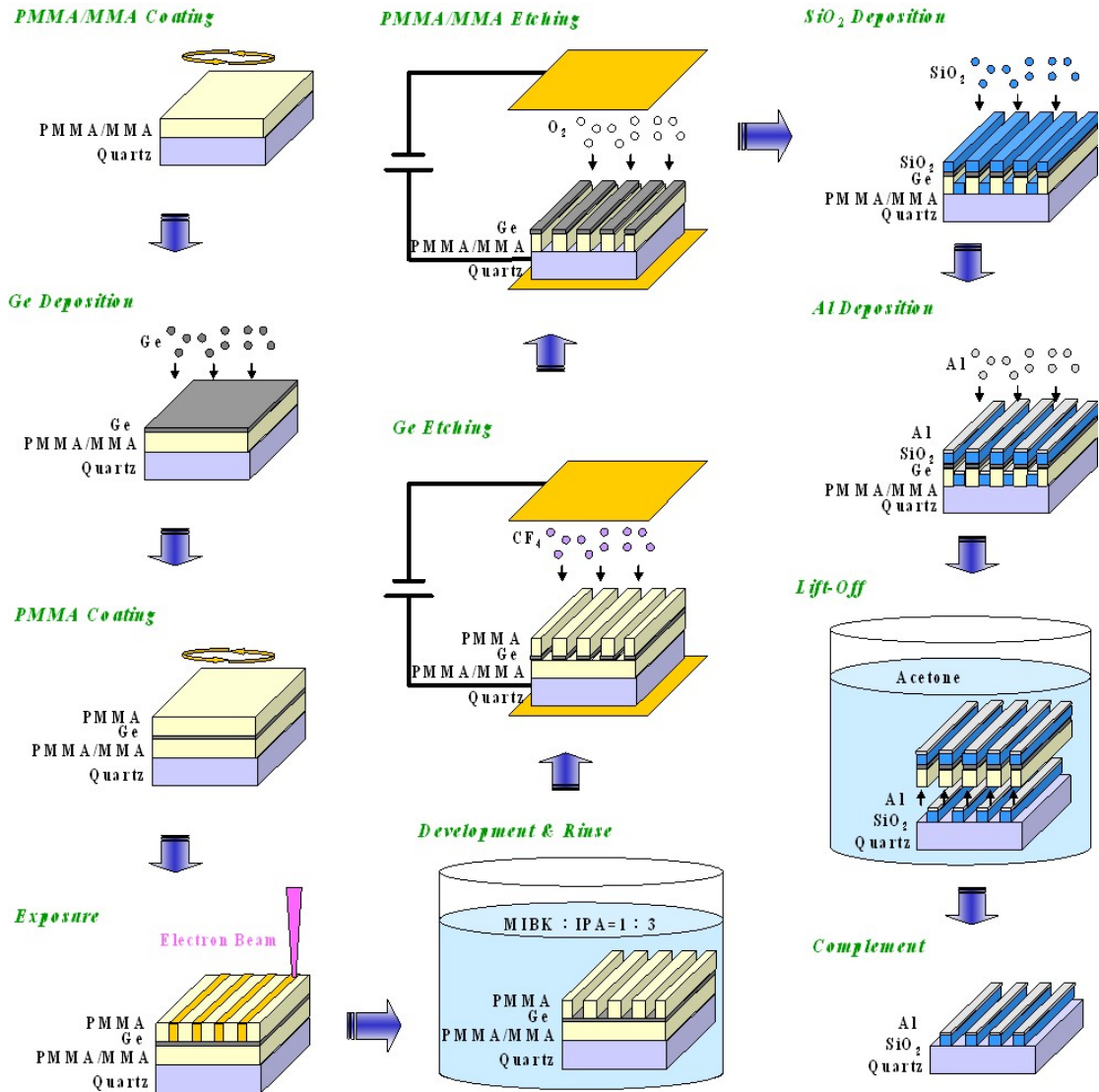
PMMA/MMA Coating

PMMA/MMA
Quartz

Ge Deposition

Ge
PMMA/MMA
Quartz

PMMA Coating

PMMA
Ge
PMMA/MMA
Quartz

Exposure

Electron Beam

PMMA
Ge
PMMA/MMA
Quartz

PMMA/MMA Etching

O_2

Ge
PMMA/MMA
Quartz

Ge Etching

CF_4

PMMA
Ge
PMMA/MMA
Quartz

Development & Rinse

MIBK : IPA = 1 : 3

PMMA
Ge
PMMA/MMA
Quartz

SiO_2 Deposition

SiO_2

SiO_2
Ge
PMMA/MMA
Quartz

Al Deposition

Al

Al
SiO_2
Ge
PMMA/MMA
Quartz

Lift-Off

Acetone

Al
SiO_2
Quartz

Complement

Al
SiO_2
Quartz

Fig. 4-13. Flow of fabricating sub-wavelength grating with double-layer structure by using tri-level resist system.

4.4.3 Double-Layered Structure by Using Inductive Coupled Plasma-Reactive Ion Etching (ICP-RIE)

ICP-RIE process, instead of tri-level resist system, could also fabricate the sub-wavelength grating with multi-layer. The basic structure of ICP-RIE was shown in Fig. 4-14. A current was applied on the coil, which would induce a magnetic field to generate a secondary inductive current by means of certain media like air, vacuum or a ferromagnetic core. The secondary inductive current then released its energy

through plasma. Therefore, ICP-RIE was a high-density-plasma system which used magnetic confinement of electrons to generate very high ion densities $\left(> 5\times10^{11}\,cm^{-3}\right)$. The structure with high aspect ratio was able to be etched by such a high ion densities. ICP-RIE was introduced into the experiment to go deep etching process with the advantage of etching structure of high aspect ratio.
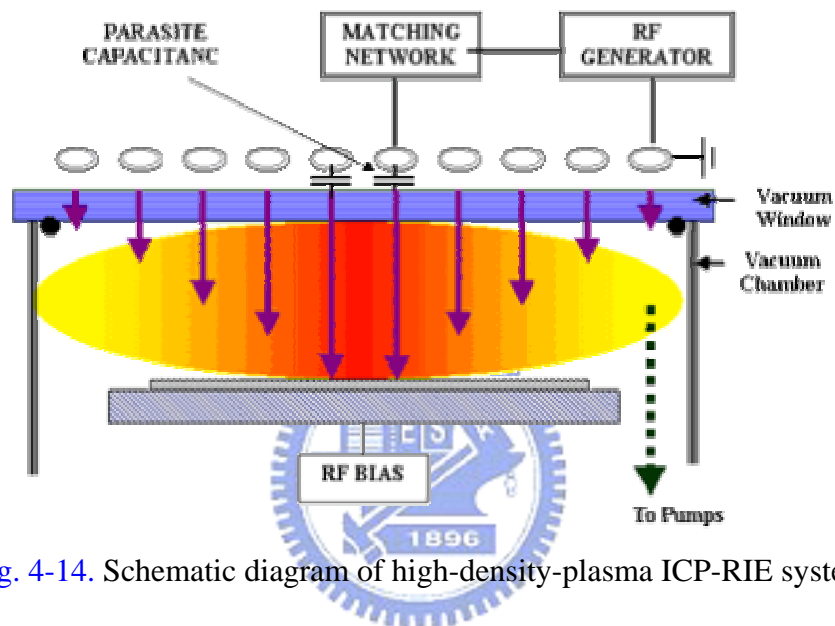

Fig. 4-14. Schematic diagram of high-density-plasma ICP-RIE system.

On the other hand, the lift-off process of a structure with high aspect ratio was not very easy to achieve. A new fabrication process by means of ICP-RIE, which was simpler than using tri-level resist system, was therefore proposed to fabricate sub-wavelength grating with double-layered structure. The detail steps were listed below：

(1) Wafer cleaning：First step was initially clean as before.

(2) Materials deposition：The desired materials were deposited on quartz first. In the experiment, SiO_2 and aluminum were applied.

(3) Resist coating：The PMMA was spin coated on aluminum after SiO_2 and aluminum were deposited.

(4) Baking：The coated PMMA was baked on a hotplate at 160°C for 15 minutes.

(5) Exposure：The wafers were then put into E-beam system to expose PMMA.

(6) Development and Rinse：The exposed PMMA was developed for 75 seconds in 1:3 MIBK：IPA and rinse for 25 seconds in IPA. Then blow dry with nitrogen.

(7) Mask deposition：The etching mask was formed on aluminum after development. The material and thickness of etching mask needed to be selected properly in order to etch structure with high aspect ratio. Here, gold was chosen due to its high etching selectivity ratio compared with aluminum and SiO_2.

(8) Lift-off：The samples were immersed into acetone for 15 minutes. Then we agitated substrates and acetone with an ultrasonic cleaner to dissolve the unexposed PMMA with its cover lift-off, and the titanium mask remained on the substrates.

(9) ICP-RIE：Then ICP-RIE with Cl_2 and CF_4 was then applied sequentially to etch Al and SiO_2 respectively and form a high aspect ratio nanostructure.

The flow of fabricating sub-wavelength grating with double layer structure by using ICP-RIE process was shown in Fig. 4-15.
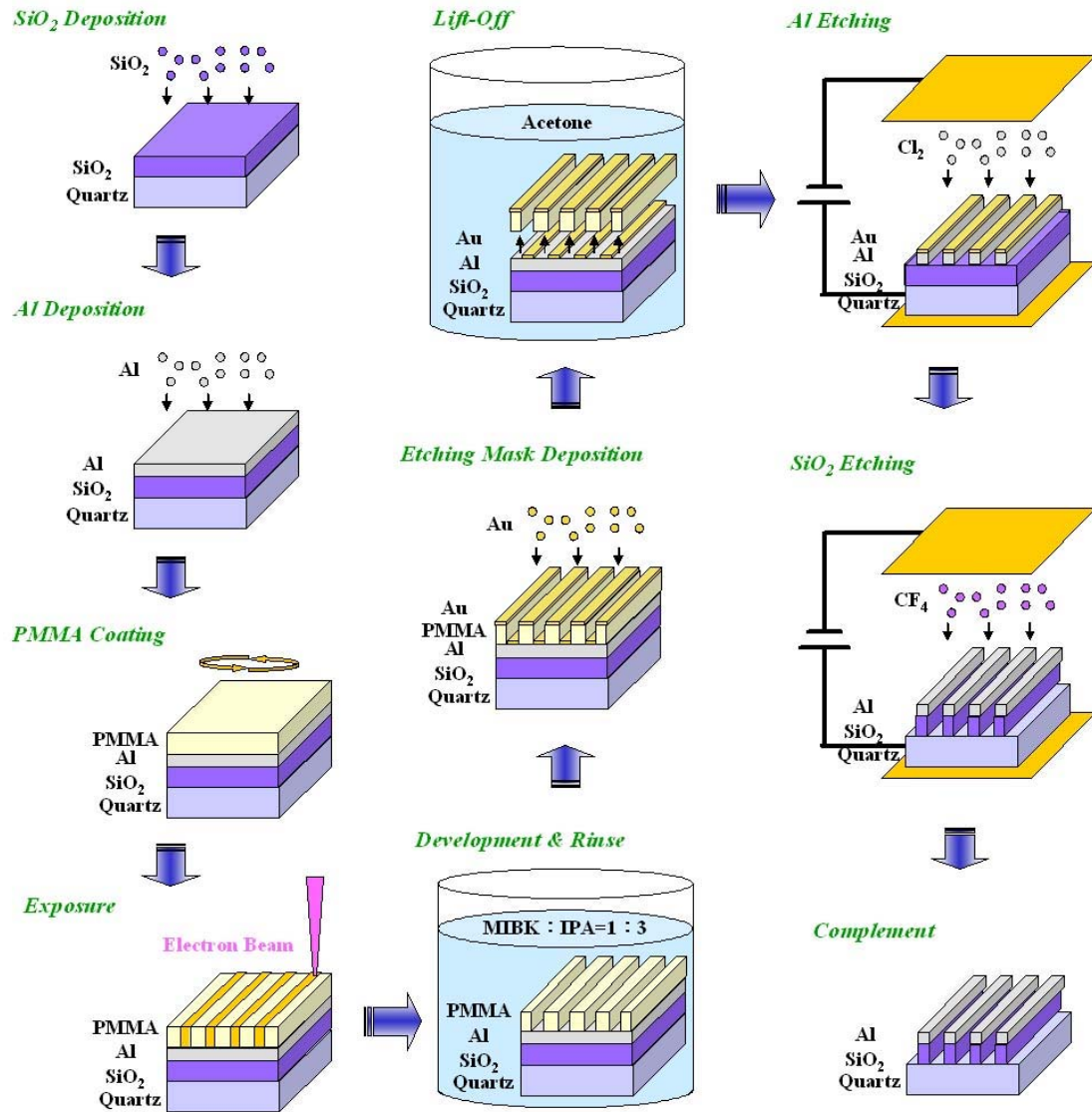
Fig. 4-15. Flow of fabricating sub-wavelength grating with double layer by using ICP-RIE process.

4.5 Measurement System

After the fabrication of sub-wavelength grating, the inspection was performed to make sure that the fabricated nanostructures are in keep with the original design. First, SEM and AFM were utilized respectively. As shown in Figs. 4-16 (a) and (b), the top view and cross section of the sub-wavelength grating with $80\,\mu m \times 80\,\mu m$ in size, $0.2\ \mu m$ in period, and $0.1\ \mu m$ in aperture size were then demonstrated.

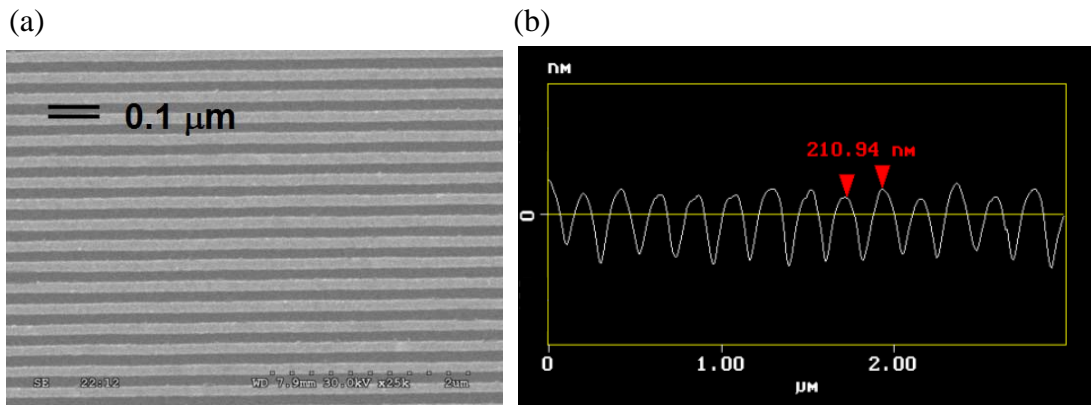(a)   (b)

Fig. 4-16. (a) Top view and (b) cross section of the fabricated sub-wavelength grating.

Besides, the experimental setup used to evaluate efficiencies of light separation will be also introduced. Because the sample size was only 80 μm × 80 μm, limited by the e-beam writer used, we therefore needed to design an experimental setup to measure the efficiency of both p-polarized light transmittance and s-polarized light reflectance. The fabricated sub-wavelength grating was evaluated by means of a setup shown schematically in Fig. 4-17.
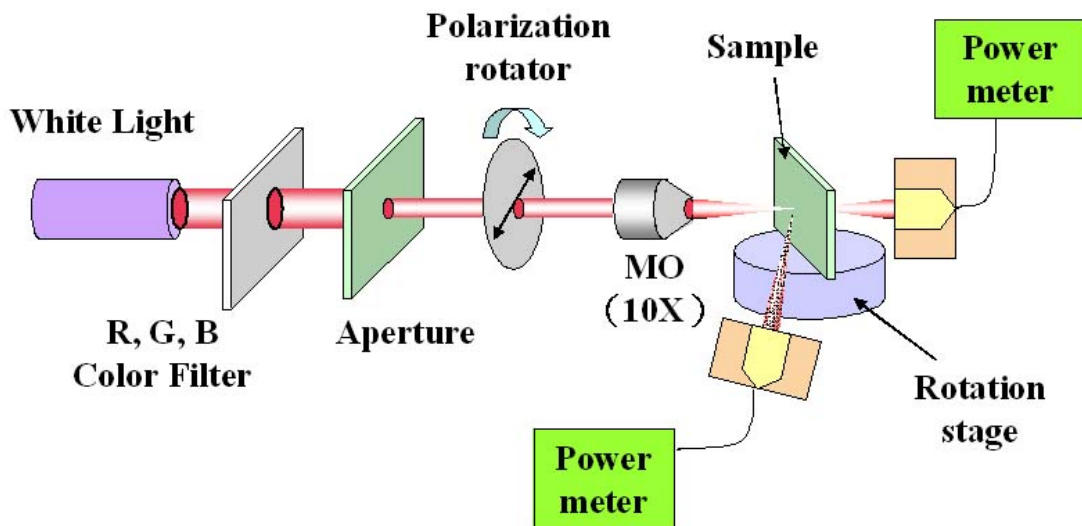

Fig. 4-17. Schematic diagram of the experimental setup for the characterization of the fabricated sub-wavelength grating.

The transmission and reflection of the fabricated sub-wavelength grating were measured using a white light source filtered with R (630 nm), G (532 nm), B (437 nm) primary wavelength color filters. The beam is focused by the microscopic objective (MO) lens to cover the entire area of the fabricated sub-wavelength grating (80 μm × 80 μm) and its input polarization is controlled by a polarization rotator. Two photodetectors were then used to measure the transmission and the reflection simultaneously. The measured and simulated reflection efficiencies versus wavelength are shown in Fig. 4-18. In such an arrangement, the measured reflection efficiencies at λ=437, 532, and 630nm are 70%, 76% and 85% for s-polarized light; transmission efficiencies for p-polarized light are 68%, 65% and 70%, respectively.
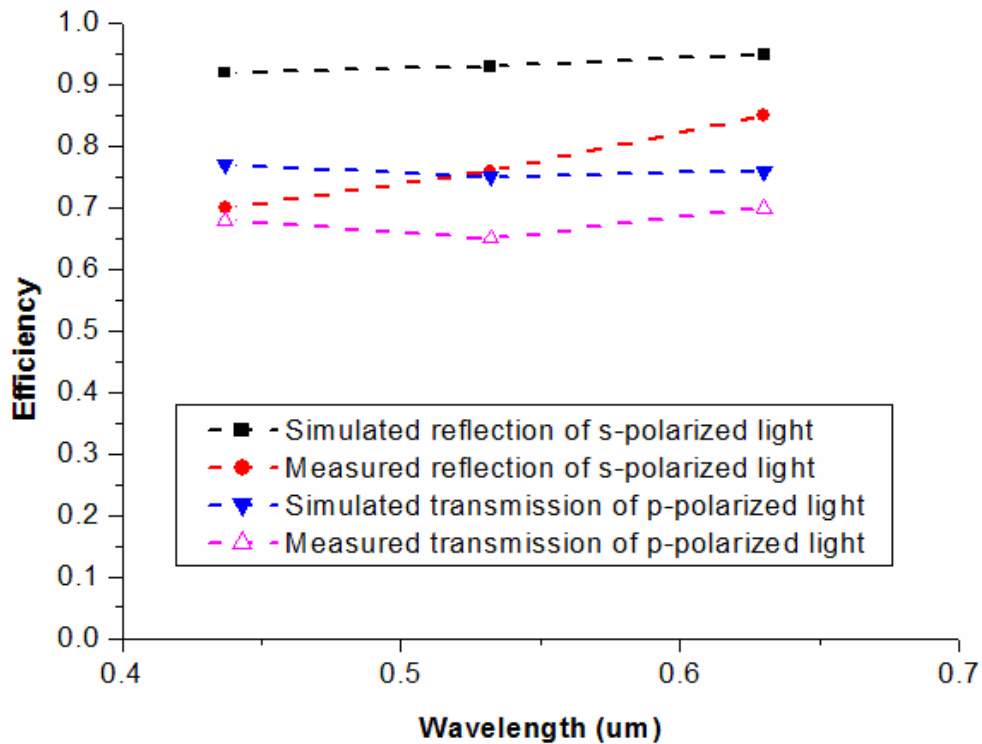

Fig. 4-18. Comparison of experimental and simulated results of the sub-wavelength grating.

Theoretically, gain factor of polarization efficiency of 2 can be achieved. In

the simulation, the transmitted p-polarized light= $P_{transmit}$+ (S convert to P)$_{transmit}$=80%×0.5+95%×0.5×0.9(quarter wave plate conversion factor)×80%=75%. For conventional backlights, the transmitted p-polarized light is about 40%. Therefore, the gain factor of polarization efficiency achieved 1.87. The gain factor difference between theoretical and simulated values was attributed to the absorption of the materials. From the simulated results shown in Fig. 4-6, we find that the gain factor can be closer to the theoretical value of 2 if the linewidth of the sub-wavelength grating can be further reduced. In our measurement, the transmitted p-polarized light= 85%×0.5+70%×0.5×0.9(quarter wave plate conversion factor)×85%=69%. The measured results demonstrated that the gain factor of 1.7 was retained.

The degradation of gain factor was caused by several issues, described as follows. A Gaussian distribution of the e-beam yielded the non-rectangular grating structure instead of a binary shape, lowering the efficiency of total transmitted p-polarized light. A uniform beam profile can be obtained by using electromagnetic lenses and smaller apertures to correct the Gaussian beam profile. Grating structures with high aspect ratio can also reduce the effects caused by non-rectangular shape. Moreover, the polarization efficiency is affected by the shape, linewidth, and layer thickness of the grating.[9] From an atomic force microscope measurement, the lateral and vertical errors of the sub-wavelength grating are 5% and 9%, respectively. We expect that more precise lift-off and etching techniques can further improve the efficiency. Additionally, depolarization arose under conditions of mixed polarized states. With a 0.1 μm linewidth, the extinction ratio of s-polarized to p-polarized light exceeds 10. Although the extinction ratio is not so high, energy absorption is much reduced while illuminated on the LCD panel. Theoretically, an extinction ratio of better than 25 can be achieved if the linewidth is further reduced. Moreover, the gain factor and the extinction ratio of s-polarized to p-polarized light can be further

improved by an alternative multi-layered configuration of the sub-wavelength grating. The alternative multi-layered structures of metallic and dielectric layers and the high aspect ratio sub-wavelength grating effectively reduced the amount of transmitted p-polarized light. However, the sub-wavelength grating with a high aspect ratio is difficult in fabrication. The fabrication issue might be solved by the proposed multi-level resist approach. Furthermore, a sub-wavelength grating of large area can be realized by tiling small area grating arrays or using nano-imprinting technology in the near future.[10]

4.6 Summary

An integrated lightguide for liquid crystal display illumination was developed with p-polarized to s-polarized light conversion and uniformity improvement. This novel element combined micro slot structures and a sub-wavelength grating on both sides of the lightguide. An integrated polarized lighguide was fabricated and evaluated for its functionality. 80% brightness uniformity and 69% polarization efficiency were achieved. Thus, a gain factor of 1.7 in polarization efficiency was achieved. Consequently, an integrated lightguide of high polarization conversion efficiency shall provide a high efficiency backlight module in a compact form for LCD illumination.

4.7 References

[1] M. F. Weber, Society Information Display (SID) Digest, p.427 (1992).

[2] Z. Pang and L. Li, Society Information Display (SID) Digest, p.916 (1999).

[3] H.J.B. Jagt, H.J. Cornelissen, D.J. Broer, and C.W.M. Bastiaansen, International Display Workshop (IDW) DIGEST, p.387 (2000).

[4] F. L. Pedrotti and L. S. Pedrotti, *Introduction to Optics*, Prentice-Hall, New Jersey,

p.356 (1993).

[5] E. B. Grann, M. G. Moharam, and D. A. Pommet, J. Opt. Soc. Am. A **11**, p.2695 (1994).

[6] S. Sinzinger and J. Jahns, *Microoptics*, Wiley-Vch, New York, p.166 (1999)

[7] A. Yariv, P. Yeh, *Optical Waves in Crystal*, John Wiley & Sons, New York (1984).

[8] F. Flory, L. Escoubas, and B. Lazarides, Appl. Opt., vol. 41, No. 16, p.3332 (2002).

[9] L. L. Soares and L. Cescato, Appl. Opt., vol. 40, No. 32, p.5906 (2001)

[10] S. K. Moore, IEEE Spectrum, Vol. 39, Issue 5, p.25 (2002)